Electrochemical fabrication of single-crystalline and polycrystalline Au nanowires: the influence of deposition parameters

2006 Nanotechnology 17 1922

(http://iopscience.iop.org/0957-4484/17/8/020)

INSTITUTE OF PHYSICS PUBLISHING NANOTECHNOLOGY
Nanotechnology **17** (2006) 1922–1926 doi:10.1088/0957-4484/17/8/020

Electrochemical fabrication of single-crystalline and polycrystalline Au nanowires: the influence of deposition parameters

J Liu[1], J L Duan[1], M E Toimil-Molares[2], S Karim[3], T W Cornelius[2], D Dobrev[2], H J Yao[1], Y M Sun[1], M D Hou[1], D Mo[1], Z G Wang[1] and R Neumann[2]

[1] Institute of Modern Physics, Chinese Academy of Sciences, Lanzhou, People's Republic of China
[2] Gesellschaft für Schwerionenforschung (GSI), Darmstadt, Germany
[3] Department of Chemistry, Philipps University, Marburg, Germany

E-mail: j.liu@impcas.ac.cn

Received 15 December 2005
Published 15 March 2006
Online at stacks.iop.org/Nano/17/1922

Abstract
We report the electrochemical growth of gold nanowires with controlled dimensions and crystallinity. By systematically varying the deposition conditions, both polycrystalline and single-crystalline wires with diameters between 20 and 100 nm are successfully synthesized in etched ion-track membranes. The nanowires are characterized using scanning electron microscopy, high resolution transmission electron microscopy, scanning tunnelling microscopy and x-ray diffraction. The influence of the deposition parameters, especially those of the electrolyte, on the nanowire structure is investigated. Gold sulfite electrolytes lead to polycrystalline structure at the temperatures and voltages employed. In contrast, gold cyanide solution favours the growth of single crystals at temperatures between 50 and 65 °C under both direct current and reverse pulse current deposition conditions. The single-crystalline wires possess a [110] preferred orientation.

1. Introduction

Research on nanowires is currently motivated by the novel size-dependent properties of nanostructures and by their promising technological applications in fields such as electronics, optoelectronics, and chemical and biological sensors [1–6]. Gold possesses, in particular, very good electrical and thermal conductivity, high ductility and chemical inertness, all these characteristics being important for the fabrication of reliable electrical nanocontacts. Thanks to its specific chemical properties, gold enables the creation of nanowires with chemically inert walls, which can be suitably modified for attaching various chemical ligands or biomolecules. Nanowires altered in this way may be used as sensors [7] or spectroscopic probes [8].

A number of different methods for producing gold nanowires have been reported up to now, comprising electroless deposition in the channels of mesoporous silica thin films [9], assembly of gold nanoparticles [10], microwave synthesis [11] and lithography [12]. However, these techniques lead in most cases to polycrystalline structures, and do not allow the control of the crystallographic properties of the wires. The maximal aspect ratio is also limited in all cases.

Since the electrical, thermal and mechanical properties of the wires depend strongly on their crystallographic and morphological characteristics, further synthesis techniques are needed to fabricate nanostructures with well-controlled crystallinity. The template method, i.e. filling the pores of a host membrane with a certain material, is suitable for this purpose. In the recent past, nanowires of various metals, semiconduc-

tors and conducting polymers have been synthesized in porous membranes by electrochemical deposition, pressure injection, chemical vapour deposition (CVD), chemical polymerization and electroless deposition [13–16]. Several kinds of templates are commonly employed, e.g. porous alumina, etched ion-track membranes and diblock-copolymers. From all possible combinations of host membranes with wire synthesis techniques, electrochemical deposition in etched ion-track membranes provides the highest flexibility. On one hand, heavy-ion irradiation and chemical etching allow the production of membranes of different materials (polymers, SiO_2 and mica, among others) with pores of controlled density, different shapes (e.g. cylindrical, conical or biconical), diameters from a few nm to several μm and aspect ratios (i.e. length over diameter) up to 10^4. On the other hand, the control of deposition parameters, namely the electrolyte, temperature T, applied voltage U and current density j, provides nanowires with well-defined crystallinity and crystallographic orientation [13, 16–18].

Here, we report the electrochemical fabrication of polycrystalline and single-crystalline gold nanowire arrays in etched ion-track membranes. The wires are cylindrical with diameters between 20 and 100 nm. We demonstrate that by systematically varying the electrodeposition conditions both polycrystalline and single-crystalline wires are successfully fabricated in a well-controlled manner. We discuss the influence of the deposition conditions on the wire structure and reveal that the electrolytes employed determine to a large extent the crystal size.

2. Experimental details

The process of fabrication of the gold nanowires consisted of several steps. First, 30 μm thick polycarbonate foils (Makrofol N, Bayer Leverkusen) were irradiated at the UNILAC linear accelerator of GSI (Darmstadt) with ^{131}Xe and ^{197}Au ions (kinetic energy 11.4 MeV u $^{-1}$, fluence 10^8–10^9 ions cm^{-2}). Prior to etching, each side of the polymer foils was exposed to UV light for 1 h to enhance the track-etching rate. In a next step, the foils were etched in a 6N NaOH solution at 50 °C for a time from 1 to 3 min to obtain cylindrical pores with diameters between 20 and 100 nm. Subsequently, a thin gold film was sputtered onto one side of the membrane and reinforced electrochemically with a copper layer using a commercial bright copper bath (Cupatier, Riedel). This layer served later as a conducting substrate–cathode, and a gold cone or a platinized titanium wire served as an anode during wire growth in the pores. The following electrolytes were employed to study their suitability and their influence on the resulting wire structure under different deposition conditions: (1) ammonium sulfite gold (I) bath (Metakem) (gold content = 15 g l^{-1}, T = 55–65 °C, j = 1–1.5 mA cm^{-2}, (2) sodium disulfitoaurate (I) Imabrite 24 bath (Schloeter Galvanotechnik) (gold content = 12.3 g l^{-1}, T = 50 °C, $j \sim 3$ mA cm^{-2}) and (3) alkaline cyanide solution, namely potassium dicyanoaurate (I) Puramet 402 bath (Doduco) (gold content = 10 g l^{-1}, T = 55 °C, $j \sim 5$ mA cm^{-2}). We applied both direct current (DC) and rectangular reverse pulses (RP). The wire deposition was monitored by recording current versus time curves. The deposition process was either stopped during growth in the pores, or continued to form caps on top of the wires. Some experiments were also carried out in an ultrasonic field.

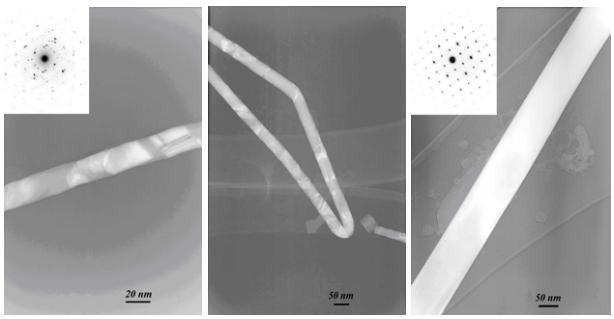

Figure 1. Bright-field HRTEM images of gold nanowires. ((a), (b)) 20 nm diameter polycrystalline wires grown in ammonium gold (I) sulfite; (c) 90 nm single-crystalline wire deposited using a cyanide electrolyte. The insets show SAED patterns.

After dissolution of the polymer membrane, the crystalline structure and morphology of the nanowires deposited at different conditions were investigated by scanning electron microscopy (SEM; Philips XL 30), high resolution transmission electron microscopy (HRTEM; JEOL JEM 4000 FX II, 400 kV) and scanning tunnelling microscopy (STM; Solver P47, NT-MDT Company). In addition, the texture of Au nanowire arrays deposited under different conditions was analysed using x-ray diffraction (XRD; RIGAKU RINT 2400, Cu Kα, λ = 1.541 78 Å) while the wires remained embedded in the membrane.

3. Results and discussion

Figures 1(a) and (b) show HRTEM images of Au nanowires deposited with ammonium gold (I) sulfite electrolyte. The bath temperature was 50 °C, and a constant voltage $U = -500$ mV was applied. Several grain boundaries are visible along the wire axis evidencing a polycrystalline structure. The HRTEM image in figure 1(c) depicts a wire deposited with cyanidic electrolyte at $U = -900$ mV and 60 °C, applying an ultrasonic field. No grain boundaries were observed in the wires grown under these conditions, indicating that they are single-crystalline. The polycrystallinity and single-crystallinity were further confirmed using selected area electron diffraction (SAED) patterns, shown as insets in figures 1(a) and (c), respectively. The pattern of the single-crystalline wires did not change on moving the electron beam along the wire.

Figures 2(a) and (b) display the diffraction patterns of the wire arrays deposited under the same conditions as the wires shown in figures 1(a) and (c), respectively. In order to quantitatively discuss the degree of orientation, we calculated the texture coefficients (TC) of each of the reflections (hkl). The texture coefficient TC$(h_ik_il_i)$ is TC$(h_ik_il_i) = \frac{I(h_ik_il_i)/I_0(h_ik_il_i)}{(1/N)\times\sum_{j=1}^{N}(I(h_jk_jl_j)/I_0(h_jk_jl_j)}$. Here, $I_0(h_ik_il_i)$ are the intensities of the $(h_ik_il_i)$ lattice plane of a standard Au power sample, $I(h_ik_il_i)$ are the intensities of the $(h_ik_il_i)$ lattice plane under analysis. N is the total number of reflection planes. For a polycrystalline sample, TC$(h_ik_il_i) = 1$ for all reflections. A TC$(h_ik_il_i) > 1$ indicates a preferred crystallographic

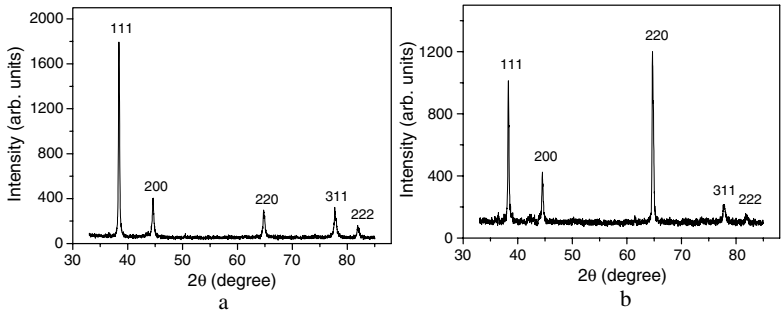

Figure 2. XRD spectra of (a) polycrystalline and (b) single-crystalline Au nanowires.

Table 1. The deposition parameters and the gold nanowire crystalline structures.

Electrolyte types	Temperatures (°C)	Voltages (V)	Gold nanowire crystalline structures
Sodium disulfitoaurate (I), 12.3 g l^{-1}, pH = 7–7.5	50–55	DC (−0.2 to −0.8)	Polycrystalline
Ammonium gold (I) sulphite, 15 g l^{-1}, pH = 7.5	50–65	DC (−0.5 to −1.0) RP (−0.4(4s)/0.1(1s)) Ultrasonic	Fine-grained polycrystalline. RP and ultrasonic improve the density and homogeneity of wires, respectively.
Potassium dicyanoaurate (I), 10 g l^{-1}, pH = 7.3	50–65	DC (−0.5 to −1.0) RP (−0.5(5s)/0.6(1s)) Ultrasonic	Single-crystalline with diameters of few ten nm under DC. Single-crystalline with diameters of hundred nm under RP.

orientation perpendicular to the $(h_i k_i l_i)$ planes. For the wires deposited from a sulfite electrolyte (figure 2(a)), TC(111) = 1.4, while the TC of the other reflections is smaller than one. This means that the wires are polycrystalline with a weak preferred orientation along the [111] direction. For the wires deposited from a cyanide electrolyte (figure 2(b)), TC(220) = 2.5 indicating a preferential growth perpendicular to the (110) plane, in good agreement with the results obtained by TEM and SAED.

When the deposition is continued once the wires reach the membrane surface, caps grow on top. We found that the caps possess different morphologies, depending on the wire crystallinity [16]. Figure 3 displays different shapes: (a) round, smooth and polycrystalline for deposition with ammonium gold (I) sulfite applying $U = -500$ mV at 50 °C, (b) polycrystalline with a rough laminar structure for deposition using a sodium gold (I) sulfite with $U = -800$ mV at 50 °C, (c) faceted, showing the single-crystalline structure when using the potassium dicyanoaurate (I) bath and applying DC ($U = -900$ mV) and (d) faceted and single-crystalline on applying reverse pulses −500 mV(5 s)/600 mV(1 s) at 60 °C. TEM, SEM and XRD results evidence a very strong dependence of the crystallinity on the electrolyte. The deposition parameters and the crystalline structures of gold nanowires are shown in table 1.

The tradition electrolytes from which to deposit gold contain gold (I) cyanide complex and non-cyanide, sulfitic-based gold depositing solution. Gold (I) cyanide complex, $[Au(CN)_2]^-$, liberates free cyanide ions during the depositing. The cathodic deposition of gold can be described by Butler–Volmer kinetics. At lower currents or less negative potentials the first step is the chemical adsorption of the $[Au(CN)_2]^-$ complex, $[Au(CN)_2]^- \rightarrow [Au(CN)]_{ad} + CN^-$. Then, $[Au(CN)]_{ad} + e^- \rightarrow [Au^0CN]^-_{ad}$. The chemical crystallization is the last step, $[Au^0CN]^-_{ad} \Leftrightarrow Au + CN^-$ [19]. In the sulfitic gold complex, $Au(SO_3)_2^{3-}$ is a primary ingredient of the depositing solution. $Au(SO_3)_2^{3-}$ decomposes into Au and sulfite ions in the solution, $Au(SO_3)_2^{3-} \Leftrightarrow Au^+ + 2SO_3^{2-}$. Free aurous ($Au^+$) combine with electrons to deposit solid gold metal into nanopores of membrane placed at the cathode, $Au^+ + e^- \rightarrow Au$. However, the sulfite bath without any stabilizing additive suffers from the instability caused by

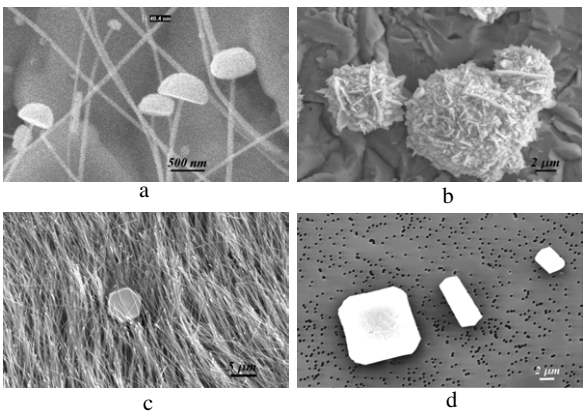

Figure 3. SEM images of caps grown on top of Au nanowires under different electrochemical conditions, displaying varying morphologies. (a) Well-defined grains of polycrystalline hemispherical caps; (b) lamina structure caps; (c) a faceted single-crystalline cap surrounded by wires after dissolving the membrane; (d) faceted single-crystalline caps before dissolving the membrane.

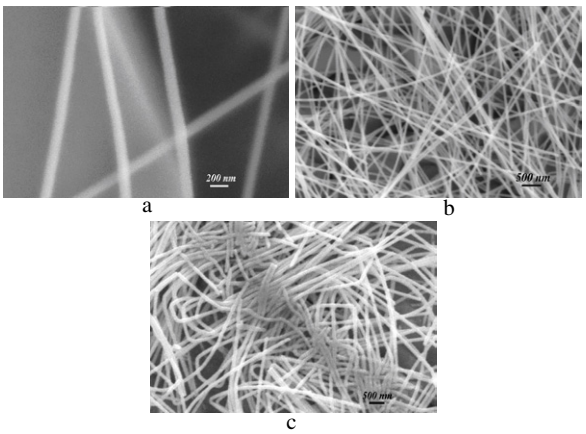

Figure 4. SEM images of Au nanowires: (a) single-crystalline; (b) and (c) polycrystalline.

the low stability constant of gold (I) sulfite complex itself, which is approximately equal to 10^{10} as compared to 10^{39} for the cyanide complex [20]. Because of the low stability constant, Au^+ ions are formed more readily from the sulfite complex, and these ions undergo a disproportionation reaction, $2Au^+ \rightarrow Au(0) + Au^{3+}$, forming a precipitate of metallic gold or colloidal gold particles during deposition, which are subsequently adsorbed and incorporated in the wires on the cathode, thus leading to the formation of polycrystalline structures. Gold deposition from sulfite-based electrolytes (both sodium disulfite and ammonium disulfite) resulted in polycrystalline wires for both DC and reverse pulse deposition, for the full range of voltages and temperatures applied in this work. We observed that nanowires deposited from ammonium disulfite gold baths possessed smaller grains than those from sodium disulfite baths. For both electrolytes, effects of the temperature on the crystallinity were not found. The use of an ultrasonic field did not significantly influence the crystallinity either, but it did improve the convection in the pores and thus the homogeneity of the growth on the whole sample, leading to homogeneous wire arrays. In contrast, applying ultrasonic fields using both DC and pulse deposition, cyanide-based electrolytes favoured the growth of single-crystalline nanowires. Single-crystalline wires with diameters of a few μm were grown at 60 °C by pulse deposition in an ultrasonic field [21], while those with diameters of a few tens of nm were successfully grown only by DC deposition, pulse deposition in this case resulting in either short and thin, or long and thick wires.

The nanowire arrays were also imaged by SEM. As evidenced in figure 4, the wires possessed in all cases cylindrical shape, and smooth and homogeneous contours. Thanks to the good quality of the polymeric templates, the diameter distribution within a given sample was also very narrow. After membrane dissolution, wires fabricated under conditions leading to single crystallinity were straight or slightly curved (figure 4(a)). Wires fabricated with sulfite electrolytes (i.e. finer grained) were straight (figure 4(b)) or sometimes mechanically bent (figure 4(c)), a change occurring during the SEM sample preparation. Similar phenomena were observed for the nanowires in TEM measurements. While single-crystalline wires mostly remained straight on the TEM grid, polycrystalline wires with diameters as small as 20 nm were bent and twisted without breaking (figure 1(b)).

Polycrystalline wires with diameter 50 nm deposited at −500 mV and 50 °C with ammonium gold (I) sulfite electrolyte (the same conditions as for the wires shown in figures 1(a) and (b)) were imaged additionally by STM as depicted in figure 5. The microscope was operated in constant-current mode using a mechanically polished Pt/Ir tip. The images reveal wires composed of many nanocrystals (grains) with sizes around 10 nm. A large number of grain boundaries are clearly visible along the wires. In addition, in figure 5(a), it is seen that one wire softly leans on another (indicated by arrows). The height profile of the dashed line AB is shown below in figure 5(a).

As the grains are downsized, the material becomes tougher by blocking dislocations more effectively. Hardness and yield stress of bulk materials typically increase with decreasing grain size. This phenomenon is called the Hall–

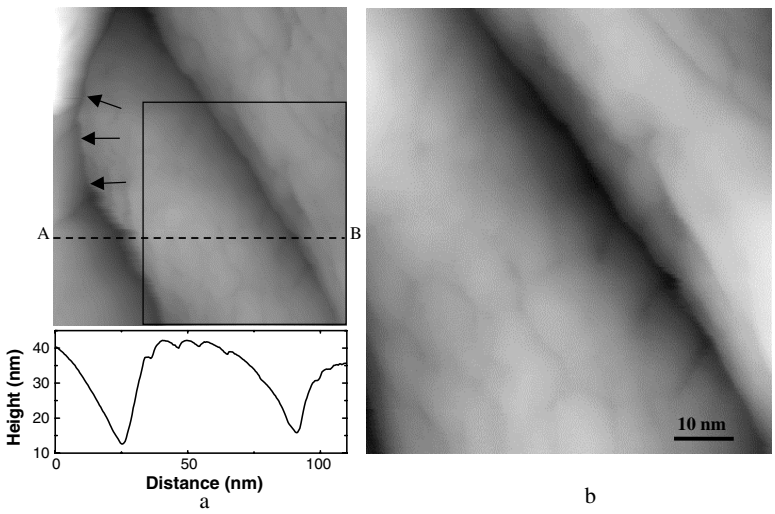

Figure 5. STM image of polycrystalline gold nanowires. The curve in (a) shows the height profile along the dashed line AB; (b) is a magnified view of the square in (a).

Petch effect [22, 23]. On the nanometre scale, however, an opposite behaviour was discovered from the computational simulations [24]. For instance, nanocrystalline copper and palladium became softer with grain size decreasing to 19.3 and 11.2 nm, respectively. As a result, the strength of a polycrystalline material first increases and then decreases with diminishing grain size. In this work, STM and TEM images indicate that the polycrystalline gold nanowires with grain sizes around 10 nm can be bent and twisted easily due to the sliding motions at grain boundaries.

In conclusion, we have found suitable deposition conditions for the controlled fabrication of both single-crystalline and polycrystalline gold nanowires. While sulfite electrolytes lead to polycrystalline structures for all temperatures and voltages employed by us, cyanide electrolyte clearly favours the potentiostatic growth of single crystals at temperatures between 50 and 65 °C. The single-crystalline wires possess a [110] preferred orientation along the wire axis.

Acknowledgments

One of the authors (JL) would like to thank the Chinese Academy of Sciences (CAS) and the Japan Society for the Promotion of Science (JSPS) for research scholarships. The authors gratefully acknowledge HRTEM support at the University of Tokyo, and financial support from the West Project of the Chinese Academy of Sciences and National Natural Science Foundation of China (10375079 and 10575125).

References

[1] Williams W D and Giordano N 1986 *Phys. Rev.* B **33** 8146
[2] Whitney T M, Jiang J S, Searson P C and Chien C L 1993 *Science* **261** 1316
[3] Blondel A, Meler J P, Doudin B and Ansermet J Ph 1994 *Appl. Phys. Lett.* **65** 3019
[4] Dubois S, Michel A, Eymery J P, Duvail J L and Piraux L 1999 *J. Mater. Res.* **14** 665
[5] Huczko A 2000 *Appl. Phys.* A **70** 365–76
[6] Xia Y, Yang P, Sun Y, Wu Y, Mayers B, Gates B, Yin Y, Kim F and Yan H 2003 *Adv. Mater.* **15** 353
[7] Yun M, Myung N V, Vasquez R P, Lee C, Menke E and Penner R M 2004 *Nano Lett.* **4** 419
[8] Mohamed M B, Volkov V, Link S and El-Sayed M A 2000 *Chem. Phys. Lett.* **317** 517
[9] Gu J L, Shi J L, Xiong L M, Chen H R, Li L and Ruan M L 2004 *Solid State Sci.* **6** 747
[10] Huang Y J, Li D and Li J H 2004 *Chem. Phys. Lett.* **389** 14
[11] Tsuji M, Hashimoto M, Nishizawa Y and Tsuji T 2004 *Mater. Lett.* **58** 2326
[12] Durkan C and Welland M E 2000 *Phys. Rev.* B **61** 14215
[13] Martin C R 1996 *Chem. Mater.* **8** 1739
[14] Zhang Z, Gekhtman D, Dresselhaus M S and Ying J Y 1999 *Chem. Mater.* **11** 1659
[15] Limmer S J, Seraji S, Forbess M J, Wu Y, Chou T P, Nguyen C and Cao G 2001 *Adv. Mater.* **13** 1269
[16] Toimil-Molares M E, Buschmann V, Dobrev D, Neumann R, Scholz R, Schuchert I U and Vetter J 2001 *Adv. Mater.* **13** 62
[17] Possin G E 1970 *Rev. Sci. Instrum.* **41** 772
[18] Toimil-Molares M E, Brötz J, Buschmann V, Dobrev D, Neumann R, Scholz R, Schuchert I U, Trautmann C and Vetter J 2001 *Nucl. Instrum. Methods* B **185** 192
[19] Chrzanowski W, Li Y G and Lasia A 1996 *J. Appl. Electrochem.* **26** 385
[20] Schlesinger M and Paunovic M 2000 *Modern Electroplating* (New York: Wiley–Interscience)
[21] Dobrev D, Vetter J, Angert N and Neumann R 2000 *Electrochim. Acta* **45** 3117
[22] Hall E O 1951 *Proc. Phys. Soc. Lond.* B **64** 747
[23] Petch N J 1953 *J. Iron Steel Inst.* **174** 25
[24] Schiøtz J, Di Tolla F D and Jacobsen K W 1998 *Nature* **391** 561